

# To investigate the impact of shell closure on $N/Z$ of $^{206-216}\text{Rn}^*$ using neutron multiplicity as a probe

Punit Dubey<sup>1,\*</sup>, Mahima Upadhyay<sup>1</sup>, Mahesh Choudhary<sup>1</sup>, Namrata Singh<sup>1</sup>, Shweta Singh<sup>1</sup>, Sriya Paul<sup>1</sup>, Nedumbally Saneesh<sup>2</sup>, Rishabh Prajapati<sup>2</sup>, Mohit Kumar<sup>2</sup>, Komalan Satheedas Golda<sup>2</sup>, Akhil Jhingan<sup>2</sup>, Pullanhiotan Sugathan<sup>2</sup>, Jhilam Sadhukhan<sup>3</sup>, Raghav Agarwal<sup>4</sup>, Kiran<sup>4</sup>, and Ajay Kumar<sup>1\*\*</sup>

<sup>1</sup>Department of Physics, Banaras Hindu University, Varanasi - 221005, India

<sup>2</sup>Inter-University Accelerator Centre, Aruna Asaf Ali Marg, New Delhi - 110067, India

<sup>3</sup>Variable Energy Cyclotron Centre, Kolkata - 700064, India

<sup>4</sup>Department of Physics, Panjab University, Chandigarh - 160014, India

**Abstract.** The fission timescale of the compound nucleus (CN)  $^{206}\text{Rn}$ , formed through the reaction  $^{28}\text{Si}+^{178}\text{Hf}$ , has been investigated using pre-scission neutron multiplicities as a diagnostic probe within the excitation energy range of 61–90 MeV. The obtained results for the  $^{206}\text{Rn}$  system have been compared with available experimental data for other radon isotopes ( $^{208,210,212,214,216}\text{Rn}$ ) to examine the influence of shell closures on the total neutron multiplicity. A distinct trend has been identified in the neutron-to-proton ( $N/Z$ ) ratio dependence, wherein the total neutron multiplicity decreases as the compound nucleus approaches shell closure and subsequently increases as it moves away from it. Furthermore, clear signatures of shell effects have been observed at excitation energies exceeding 50 MeV; an energy regime where such effects were not reported in earlier investigations.

## 1 Introduction

To investigate the underlying nuclear dynamics governing low-energy heavy-ion collisions, a range of experimental observables are employed, including measurements of fragment mass, total kinetic energy (TKE), particle multiplicities, angular distributions of fission fragments, and their mutual correlations. Among these, the pre-scission neutron multiplicity ( $M_{\text{pre}}$ ) has emerged as one of the most effective probes for assessing the fission timescale in heavy-ion-induced fusion–fission (HIFF) reactions [1]. This efficacy arises from the fact that neutrons emitted from the compound nucleus prior to scission are kinematically distinct from those emitted by the fission fragments, thereby enabling precise determination of their multiplicity. Experimental observations have consistently revealed pre-scission neutron multiplicities significantly exceeding the predictions of conventional statistical models describing compound nucleus decay [1, 2]. Analogous deviations have also been reported for pre-scission light charged particles [3] and Giant Dipole Resonance (GDR)  $\gamma$ -rays [4]. Extensive experimental investigations employing diverse projectile–target combinations [5–24] have been conducted to elucidate the influence of entrance-channel dynamics, shell effects,  $N/Z$ , excitation energy, and other relevant physical parameters on these phenomena. Nuclear dissipation significantly influences the dynamics of HIFF. Studies across the various mass regions highlight its role, along with entrance-channel ef-

fects, in shaping nuclear evolution and compound nucleus formation [9–13, 16, 25–31]. In particular, the entrance-channel mass asymmetry,  $\alpha = (A_t - A_p)/(A_t + A_p)$ , serves as a key parameter governing the dynamical progression of the dinuclear system.

Further investigations revealed that dissipation is relatively weaker in shell-closed nuclei compared to neighboring open-shell systems [7, 29, 32]. Studies also suggest that with increasing excitation energy, the shell effect on  $M_{\text{pre}}$  weakens progressively [9, 32]. In our recent investigation, it was observed that below the shell closure, the dissipation within the compound nucleus exhibits an increasing trend with rising excitation energy. At the shell closure, the dissipation remains nearly constant with further increase in excitation energy, whereas beyond the shell closure, it gradually decreases as the excitation energy continues to rise [30]. Only limited experimental and theoretical studies have explored the impact of  $N/Z$  on pre-scission neutron multiplicity in the past. W. Ye [33] reported that  $M_{\text{pre}}$  increases with an increase in  $N/Z$ , whereas Sandal *et al.* [9] observed no distinct trend in dissipation strength with respect to  $N/Z$ .

In this study, we first correlated our experimental results with shell closure systematics, along with existing experimental data on neutron multiplicities. We then compared our observations with predictions from a dynamical model code [34] to estimate the fission time scale. Additionally, we evaluated the influence of shell closure on the  $N/Z$  ratio for the present measurements and compared these results with available data reported in the literature.

\*e-mail: punitdubey@bhu.ac.in

\*\*e-mail: ajaytyagi@bhu.ac.in

**Table 1.** Details of the reactions used in this work.

S. No.	CN	Reaction	$\delta_{sh}$	Ref.	S. No.	CN	Reaction	$\delta_{sh}$	Ref.
1a	$^{243}\text{Am}$	$^{11}\text{B}+^{232}\text{Th}$	19	[5]	5b	$^{200}\text{Pb}$	$^{19}\text{F}+^{181}\text{Ta}$	-24	[8]
1b	$^{248}\text{Cf}$	$^{11}\text{B}+^{237}\text{Np}$	24	[5]	5c	$^{203}\text{Bi}$	$^{19}\text{F}+^{184}\text{W}$	-21	[22]
2a	$^{206}\text{Po}$	$^{12}\text{C}+^{194}\text{Pt}$	-18	[6]	5d	$^{213}\text{Fr}$	$^{19}\text{F}+^{194}\text{Pt}$	-11	[7]
2b	$^{210}\text{Po}$	$^{12}\text{C}+^{198}\text{Pt}$	-14	[6]	5e	$^{215}\text{Fr}$	$^{19}\text{F}+^{196}\text{Pt}$	-9	[7]
2c	$^{216}\text{Ra}$	$^{12}\text{C}+^{204}\text{Pb}$	-8	[11]	5f	$^{216}\text{Ra}$	$^{19}\text{F}+^{197}\text{Au}$	-8	[11]
2d	$^{244}\text{Cm}$	$^{12}\text{C}+^{232}\text{Th}$	20	[5]	5g	$^{217}\text{Fr}$	$^{19}\text{F}+^{198}\text{Pt}$	-7	[7]
3a	$^{197}\text{Tl}$	$^{16}\text{O}+^{181}\text{Ta}$	-27	[12]	5h	$^{228}\text{U}$	$^{19}\text{F}+^{209}\text{Bi}$	4	[13]
3b	$^{210}\text{Rn}$	$^{16}\text{O}+^{194}\text{Pt}$	-14	[9]	5i	$^{251}\text{Es}$	$^{19}\text{F}+^{232}\text{Th}$	27	[8]
3c	$^{213}\text{Fr}$	$^{16}\text{O}+^{197}\text{Au}$	-11	[8]	6a	$^{229}\text{Np}$	$^{20}\text{Ne}+^{209}\text{Bi}$	5	[17]
3d	$^{214}\text{Rn}$	$^{16}\text{O}+^{198}\text{Pt}$	-10	[9]	7a	$^{198}\text{Rb}$	$^{28}\text{Si}+^{170}\text{Er}$	-24	[18]
3e	$^{220}\text{Th}$	$^{16}\text{O}+^{204}\text{Pb}$	-4	[14]	7b	$^{206}\text{Rn}$	$^{28}\text{Si}+^{178}\text{Hf}$	-18	present work
3f	$^{222}\text{Th}$	$^{16}\text{O}+^{206}\text{Pb}$	-2	[14]	8a	$^{200}\text{Pb}$	$^{30}\text{Si}+^{170}\text{Er}$	-22	[18]
3g	$^{224}\text{Th}$	$^{16}\text{O}+^{208}\text{Pb}$	0	[14]	8b	$^{208}\text{Rn}$	$^{30}\text{Si}+^{178}\text{Hf}$	-16	[10]
3h	$^{248}\text{Cf}$	$^{16}\text{O}+^{232}\text{Th}$	24	[5]	8c	$^{212}\text{Ra}$	$^{30}\text{Si}+^{182}\text{W}$	-12	[19]
4a	$^{202}\text{Pb}$	$^{18}\text{O}+^{184}\text{W}$	-22	[15]	8d	$^{214}\text{Ra}$	$^{30}\text{Si}+^{184}\text{W}$	-10	[19]
4b	$^{204}\text{Pb}$	$^{18}\text{O}+^{186}\text{W}$	-20	[16]	8e	$^{216}\text{Ra}$	$^{30}\text{Si}+^{186}\text{W}$	-8	[19]
4c	$^{210}\text{Po}$	$^{18}\text{O}+^{192}\text{Os}$	-14	[8]	8f	$^{227}\text{Np}$	$^{30}\text{Si}+^{197}\text{Au}$	5	[20]
4d	$^{212}\text{Rn}$	$^{18}\text{O}+^{194}\text{Pt}$	-12	[9]	9a	$^{216}\text{Th}$	$^{32}\text{S}+^{184}\text{W}$	-8	[13]
4e	$^{216}\text{Rn}$	$^{18}\text{O}+^{198}\text{Pt}$	-8	[9]	9b	$^{230}\text{Pu}$	$^{32}\text{S}+^{198}\text{Pt}$	4	[23]
5a	$^{197}\text{Tl}$	$^{19}\text{F}+^{178}\text{Hf}$	-27	[12]	10a	$^{208}\text{Rn}$	$^{48}\text{Ti}+^{160}\text{Gd}$	-16	[10]

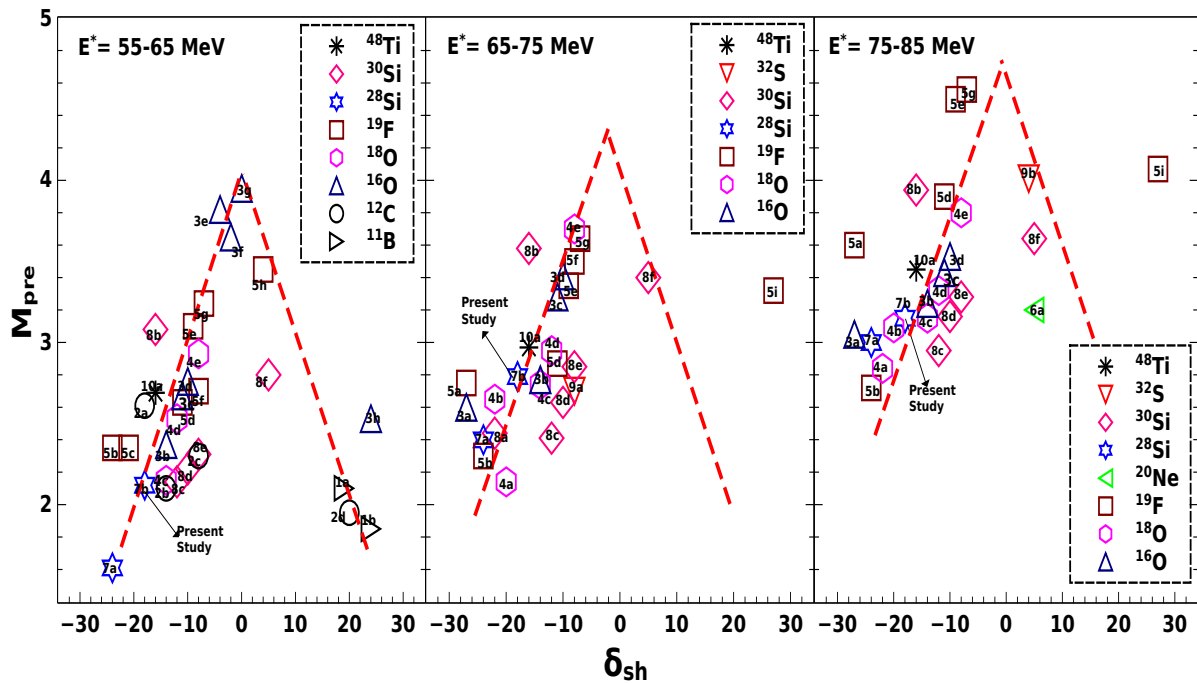


**Figure 1.** Variation of available experimental data of  $M_{pre}$ , including present data (7b), with  $\delta_{sh}$  in three different energy regions. The errors in  $M_{pre}$  lies within the height of the symbols. Alpha-numeric value in each symbol corresponds to the reactions serial number in Table 1. (Dashed lines are drawn to guide the eye.)

## 2 Discussions

### 2.1 Systematics of pre-scission neutron multiplicity

We compare the available  $M_{pre}$  data, including the present measurements, for 40 reactions spanning the compound nucleus mass range of  $197 \leq A_{CN} \leq 251$ . The details of these reactions are listed in Table 1. To minimize the influence of excitation energy, all data are categorized into three distinct  $E^*$  intervals: 55–65 MeV, 65–75 MeV, and 75–85 MeV. For certain reactions, multiple data points exist within a 10 MeV energy window; however, since  $M_{pre}$  exhibits minimal variation over this range, a representative value near the midpoint of the interval is selected.

Here,  $\delta_{sh}$  is defined as the sum of the deviations of the proton and neutron numbers of the projectile and target from selected reference shell closures. In the present work, the reference reaction  $^{16}\text{O} + ^{208}\text{Pb}$  is adopted, as both nuclei are doubly magic and a large fraction of the available experimental data in the literature are clustered around systems involving projectiles close to  $^{16}\text{O}$  and targets near  $^{208}\text{Pb}$ , rather than around other doubly magic nuclei such as  $^{40}\text{Ca}$  or  $^{132}\text{Sn}$ .

We emphasize that the choice of reference is therefore guided by consistency across the dataset, rather than by identifying the nearest shell closure for each individual nucleus. The sign of  $\delta_{sh}$  is kept to show whether there is an excess or a deficit of nucleons compared to the reference configuration, since both cases can affect the dynamics differently. This also helps ensure a consistent comparison across all reactions in Table 1. As an illustrative example, for the  $^{28}\text{Si} + ^{178}\text{Hf}$  reaction, the deviations of neutron and proton numbers of the projectile with respect to the reference nucleus  $^{16}\text{O}$  are given by

$$(\delta_{sh})_{proj,neut} = N_{^{28}\text{Si}} - N_{^{16}\text{O}} = 14 - 8 = 6 \quad (1)$$

$$(\delta_{sh})_{proj,prot} = Z_{^{28}\text{Si}} - Z_{^{16}\text{O}} = 14 - 8 = 6 \quad (2)$$

Similarly, for the target relative to  $^{208}\text{Pb}$ , the corresponding deviations are

$$(\delta_{sh})_{targ,neut} = N_{^{178}\text{Hf}} - N_{^{208}\text{Pb}} = 106 - 126 = -20 \quad (3)$$

$$(\delta_{sh})_{targ,prot} = Z_{^{178}\text{Hf}} - Z_{^{208}\text{Pb}} = 72 - 82 = -10 \quad (4)$$

Summing all four contributions yields  $\delta_{sh} = -18$ . Thus,  $\delta_{sh}$  serves as a cumulative measure of the deviation of a given projectile–target system from the chosen closed shell reference configuration. In this work, the sign of each contribution is explicitly retained, rather than using absolute values, in order to distinguish between an excess and a deficit of nucleons relative to the reference, as these may influence the reaction dynamics differently.

The dependence of  $M_{pre}$  on  $\delta_{sh}$  is presented in Fig. 1 for the three excitation energy intervals defined earlier. From figure 1, we observe a clear trend, the  $M_{pre}$  value reaches a maximum at near  $\delta_{sh} = 0$  and then decreases sharply and almost symmetrically on both sides, particularly in the 55–65 MeV energy range. The present experimental data (set 7b) are consistent with

**Table 2.** Dynamical model calculated results for  $^{28}\text{Si} + ^{178}\text{Hf}$  reaction at various excitation energies,  $\beta$  and  $\tau_{fission}$ .

$E^*$ (MeV)	$M_{pre}$	$\beta$ (MeV/ $\hbar$ )	$\tau_{fission}$ (seconds)
61.0	2.11	2.05	$(37 \pm 5) \times 10^{-21}$
71.7	2.81	4.65	$(50 \pm 5) \times 10^{-21}$
79.0	3.15	6.05	$(66 \pm 5) \times 10^{-21}$
90.0	3.36	6.20	$(67 \pm 5) \times 10^{-21}$

this behavior across all the energy intervals. However, the relative scarcity of data in the  $\delta_{sh} > 0$  region calls for further experimental investigations, especially in the higher excitation energy ranges.

### 2.2 Fission-timescale calculations

In the present investigation, the characteristic timescale of nuclear fission has been evaluated through a comprehensive dynamical model employing the stochastic Langevin equation. This formalism facilitates the description of the complete time-dependent evolution of an excited compound nucleus, beginning from its equilibrium ground-state configuration and progressing continuously until the occurrence of scission. The Langevin approach inherently accounts for both deterministic and stochastic forces acting on the nuclear collective degrees of freedom, thereby enabling a realistic simulation of the dissipative dynamics governing the fission process. Detailed theoretical formulations and computational implementations of this model are discussed extensively in Refs. [30, 34].

Within the framework of this model, the emission of neutrons from both the fissioning system and its post-scission fragments has been systematically analyzed. For each specified projectile energy, the pre-scission neutron multiplicity ( $M_{pre}$ ) was determined by performing statistical averaging over an ensemble of  $10^6$  independent Langevin trajectories. This ensemble averaging ensures an accurate representation of the inherent stochastic fluctuations and the broad distribution of fission observables associated with nuclear dissipation and diffusion effects.

The calculations were conducted by treating the shape-independent reduced dissipation coefficient ( $\beta$ ) as a variable control parameter in order to explore its influence on the fission dynamics. The fission timescale was subsequently extracted using the variable dissipation parameter approach, allowing for the investigation of the correlation between the dissipation strength and the system's intrinsic excitation energy. The obtained results reveal a pronounced increase in both the dissipation coefficient ( $\beta$ ) and the corresponding fission time as the excitation energy of the compound system increases. This trend suggests enhanced coupling between intrinsic and collective degrees of freedom at higher excitation energies, leading to a delayed scission process. The quantitative results of these calculations are summarized in Table 2 and graphically represented in Figure 2.

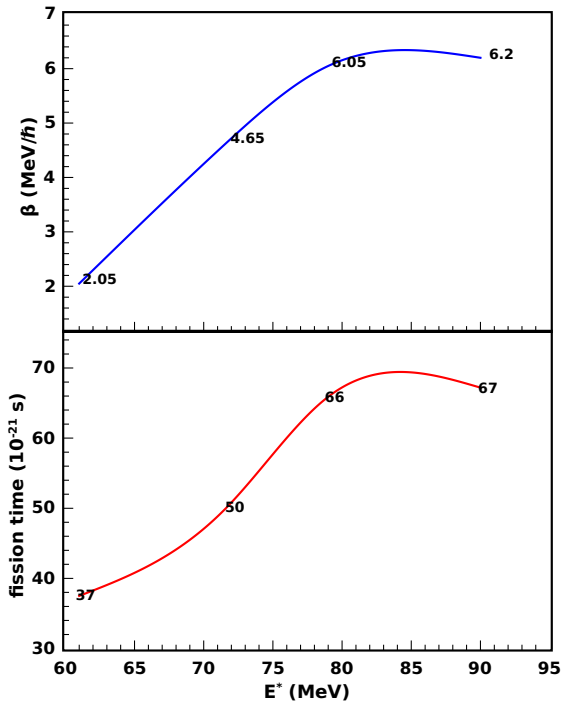


**Figure 2.** Variation in dissipation parameter  $\beta$  (top) and fission time (bottom) w.r.t. excitation energy for  $^{28}\text{Si}+^{178}\text{Hf}$  forming  $^{206}\text{Rn}$ .

### 2.3 Impact of $N/Z$ on neutron multiplicity around shell closure

In this study, we also evaluate the neutron-to-proton ( $N/Z$ ) ratio in relation to the total neutron multiplicity ( $M_{\text{total}}$ ). Our objective is to examine the variation of total neutron multiplicity as the  $N/Z$  of the compound nucleus changes. In the present work, the compound nucleus  $^{206}\text{Rn}$  is formed, while  $^{208}\text{Rn}$  is populated via the reactions  $^{30}\text{Si} + ^{178}\text{Hf}$  and  $^{48}\text{Ti} + ^{160}\text{Gd}$  [10]. Furthermore, the compound nuclei  $^{210,212,214,216}\text{Rn}$  are produced through the reactions  $^{16,18}\text{O} + ^{194,198}\text{Pt}$  [9]. A comparative analysis of the total neutron multiplicity ( $M_{\text{total}}$ ) is carried out at three excitation energies: 61.0, 71.7, and 79.0 MeV. These excitation energies were selected to correspond closely to the formation of the compound nuclei  $^{210,212,214,216}\text{Rn}$ , thereby enabling a systematic examination of isotopic trends in the fission dynamics. For  $^{208}\text{Rn}$ , the nearest attainable energy values were utilized to maintain consistency in the comparative framework. Figure 3 depicts the variation of  $M_{\text{total}}$  as a function of the  $N/Z$  of the fissioning system [30]. A distinct correlation is observed, wherein the total neutron multiplicity exhibits a pronounced increase as the system departs from the shell closure, irrespective of whether the deviation occurs toward neutron-deficient or neutron-rich isotopes. This behavior suggests that the weakening of shell effects at these regions facilitates enhanced neutron emission during the fission process. Conversely, at or near the shell closure, a marked suppression in neutron multiplicity is evident, independent of the excitation energy.

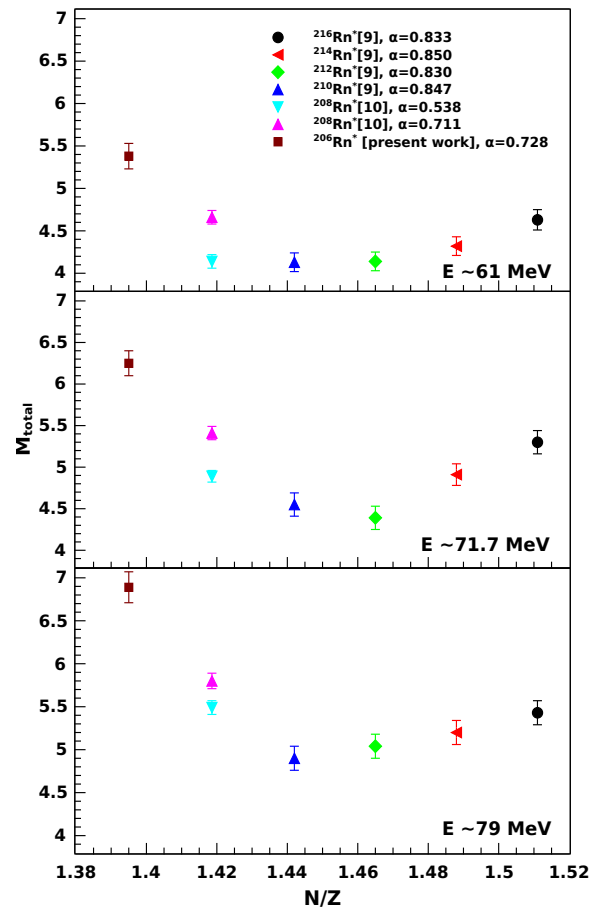


**Figure 3.** Variation of  $M_{\text{total}}$  w.r.t.  $N/Z$  ratio for compound nucleus  $^{206,208,210,212,214,216}\text{Rn}$  at excitation energies of 61.0 MeV, 71.7 MeV and 79.0 MeV [30].

## 3 Conclusion

In summary, the experimental results were compared with the shell-closure systematics and found to be in good agreement. The fission timescales, evaluated using a Langevin-based dynamical model, exhibit an increasing trend with excitation energy, indicating a gradual slowing of the fission process at higher energies. Additionally, the dependence of the total neutron multiplicity on the neutron-to-proton ratio ( $N/Z$ ) was examined for the compound nuclei  $^{206,208,210,212,214,216}\text{Rn}$ . A distinct trend was observed: the total neutron multiplicity decreases near the shell closure but increases on both the neutron-deficient and neutron-rich sides. This behavior underscores the significant role of shell effects in governing neutron emission and fission dynamics in radon isotopes.

## Acknowledgement

One of the authors (Punit Dubey) is grateful to the Prime Minister Research Fellowship (PMRF) and IoE, BHU (International travel grant) for the financial support for this work. One of the authors (Ajay Kumar) would like to thank the Institutions of Eminence (IoE) BHU [Grant No. 6031-B].

## References

- [1] D. Hilscher and H. Rossner, Dynamics of nuclear fission, *Ann. Phys. Fr.* **17**, (2), 471 (1992). <https://doi.org/10.1051/anphys:01992001706047100>
- [2] J. Cabrera, Th. Keutgen, Y. El Masri, Ch. Dufauquez, V. Roberfroid, I. Tilquin, J. VanMol, R. Regimbart, R. J. Charity *et al.*, Fusion-fission and fusion-evaporation processes in  $^{20}\text{Ne}+^{159}\text{Tb}$  and  $^{20}\text{Ne}+^{169}\text{Tm}$  interactions between  $E/A=8$  and 16 MeV, *Phys. Rev. C* **68**, 034613 (2003). <https://doi.org/10.1103/PhysRevC.68.034613>
- [3] J.P. Lestone, Determination of the time evolution of fission from particle emission, *Phys. Rev. Lett.* **70**, 2245 (1993). <https://doi.org/10.1103/PhysRevLett.70.2245>
- [4] I. Diószegi, N. P. Shaw, I. Mazumdar, A. Hatzikoutelis, and P. Paul, Nuclear viscosity of hot rotating  $^{224}\text{Th}$ , *Phys. Rev. C* **61**, 024613 (2000). <https://doi.org/10.1103/PhysRevC.61.024613>
- [5] A. Saxena, A. Chatterjee, R. K. Choudhury, S. S. Kapoor, and D. M. Nadkarni, Entrance channel effects in the fusion-fission time scales from studies of prescission neutron multiplicities, *Phys. Rev. C* **49**, 932 (1994). <https://doi.org/10.1103/PhysRevC.49.932>
- [6] K. S. Golda, A. Saxena, V. K. Mittal, K. Mahata, P. Sugathan, A. Jhingan, V. Singh, R. Sandal, S. Goyal, J. Gehlot *et al.*, Determination of shell correction energies at saddle point using pre-scission neutron multiplicities, *Nucl. Phys. A* **913**, 157 (2013). <https://doi.org/10.1016/j.nuclphysa.2013.05.016>
- [7] V. Singh, B. R. Behera, M. Kaur, A. Kumar, P. Sugathan, K. S. Golda, A. Jhingan, M. B. Chatterjee, R. K. Bhowmik, D. Siwal *et al.*, Neutron multiplicity measurements for  $^{19}\text{F}+^{194,196,198}\text{Pt}$  systems to investigate the effect of shell closure on nuclear dissipation, *Phys. Rev. C* **87**, 064601 (2013). <https://doi.org/10.1103/PhysRevC.87.064601>
- [8] D. J. Hinde, R. J. Charity, G. S. Foote, J. R. Leigh, J. O. Newton, S. Ogaza, and A. Chatterjee, Neutron multiplicities in heavy-ion-induced fission: Timescale of fusion-fission, *Nucl. Phys. A* **452**, 550 (1986). [https://doi.org/10.1016/0375-9474\(86\)90214-9](https://doi.org/10.1016/0375-9474(86)90214-9)
- [9] R. Sandal, B. R. Behera, V. Singh, M. Kaur, A. Kumar, G. Singh, K. P. Singh, P. Sugathan, A. Jhingan, K. S. Golda *et al.*, Effect of  $N/Z$  in pre-scission neutron multiplicity for  $^{16,18}\text{O}+^{194,198}\text{Pt}$  systems, *Phys. Rev. C* **87**, 014604 (2013). <https://doi.org/10.1103/PhysRevC.87.014604>
- [10] N. Kumar, S. Verma, S. Mohsina, J. Sadhukhan, K. R. Devi, A. Banerjee, N. Saneesh, M. Kumar, R. Mahajan, M. Thakur *et al.*, Probing entrance channel effects in fusion-fission dynamics through neutron multiplicity measurement of  $^{208}\text{Rn}$ , *Phy. Lett. B* **814**, 136062 (2021). <https://doi.org/10.1016/j.physletb.2021.136062>
- [11] H. Singh, K. S. Golda, S. Pal, Ranjeet, R. Sandal, B. R. Behera, G. Singh, A. Jhingan, R. P. Singh, P. Sugathan *et al.*, Role of nuclear dissipation and entrance channel mass asymmetry in pre-scission neutron multiplicity enhancement in fusion-fission reactions, *Phys. Rev. C* **78**, 024609 (2008). <https://doi.org/10.1103/PhysRevC.78.024609>
- [12] H. Singh, A. Kumar, B. R. Behera, I. M. Govil, K. S. Golda, P. Kumar, A. Jhingan, R. P. Singh, P. Sugathan, M. B. Chatterjee *et al.*, Entrance channel effects in fission of  $^{197}\text{Tl}$ , *Phys. Rev. C* **76**, 044610 (2007). <https://doi.org/10.1103/PhysRevC.76.044610>
- [13] H. Singh, B. R. Behera, G. Singh, I. M. Govil, K. S. Golda, A. Jhingan, R. P. Singh, P. Sugathan, M. B. Chatterjee, S. K. Datta *et al.*, Measurement of neutron multiplicity from fission of  $^{228}\text{U}$  and nuclear dissipation, *Phys. Rev. C* **80**, 064615 (2009). <https://doi.org/10.1103/PhysRevC.80.064615>
- [14] K. Chakraborty, M. T. Senthil Kannan, J. Sadhukhan, and S. Mandal, Systematic study of prescission neutron multiplicity: Revealing the role of entrance channel magicity, *Phy. Lett. B* **843**, 138021 (2023). <https://doi.org/10.1016/j.physletb.2023.138021>
- [15] N. K. Rai, A. Gandhi, M. T. Senthil Kannan, S. K. Roy, N. Saneesh, M. Kumar, G. Kaur, D. Arora, K. S. Golda, A. Jhingan *et al.*, Inference on fission timescale from neutron multiplicity measurement in  $^{18}\text{O}+^{184}\text{W}$ , *J. Phys. G: Nucl. Part. Phys.* **49**, 035103 (2022). <https://doi.org/10.1088/1361-6471/ac4b3f>
- [16] N. K. Rai, A. Gandhi, A. Kumar, N. Saneesh, M. Kumar, G. Kaur, A. Parihari, D. Arora, K. S. Golda, A. Jhingan *et al.*, Measurement of neutron multiplicity to investigate the role of entrance channel parameters on the nuclear dissipation, *Phys. Rev. C* **100**, 014614 (2019). <https://doi.org/10.1103/PhysRevC.100.014614>
- [17] D. J. Hinde, H. Ogata, M. Tanaka, T. Shimoda, N. Takahashi, A. Shinohara, S. Wakamatsu, K. Katori and H. Okamura, Systematics of fusion-fission time scales, *Phys. Rev. C* **39**, 2268 (1989). <https://doi.org/10.1103/PhysRevC.39.2268>
- [18] J. O. Newton, D. J. Hinde, R. J. Charity, J. R. Leigh, J. J. M. Bokhorst, A. Chatterjee, G. S. Foote and S. Ogaza, Measurement and statistical model analysis of pre-fission neutron multiplicities, *Nucl. Phys. A* **483**, 126 (1988). [https://doi.org/10.1016/0375-9474\(88\)90068-1](https://doi.org/10.1016/0375-9474(88)90068-1)
- [19] M. Shareef, E. Prasad, A. Jhingan, N. Saneesh, S. Pal, A. M. Vinodkumar, K. S. Golda, M. Kumar, A. Shamlath, P. V. Laveen *et al.*, Neutron multiplicity measurement and investigation of nuclear dissipation and shell effects in  $^{30}\text{Si}+^{182,184,186}\text{W}$  reactions, *Phys. Rev. C* **107**, 054619 (2023). <https://doi.org/10.1103/PhysRevC.107.054619>
- [20] M. Shareef, E. Prasad, A. Jhingan, N. Saneesh, K. S. Golda, A. M. Vinodkumar, M. Kumar, A. Shamlath, P. V. Laveen, A. C. Visakh *et al.*, Nuclear dissipation at high excitation energy and angular momenta in reaction forming  $^{227}\text{Np}$ , *Phys. Rev. C* **99**, 024618 (2019). <https://doi.org/10.1103/PhysRevC.99.024618>
- [21] P. N. Patil, N.M. Badiger, B. K. Nayak, S. Santra, P. C. Rout, A. Pal, G. Mohanto, K. Mahata, K. Ramachandran, R. G. Thomas *et al.*, Pre-scission neutron multiplicity in the  $^{32}\text{S}+^{184}\text{W}$  reaction, *Phys. Rev. C* **102**, 034618 (2020). <https://doi.org/10.1103/PhysRevC.102.034618>

- [22] I. Mukul, S. Nath, K. S. Golda, A. Jhingan, J. Gehlot, E. Prasad, S. Kalkal, M. B. Naik, T. Banerjee, T. Varughese *et al.*, Probing fusion-fission dynamics in  $^{203}\text{Bi}$ , *Phys. Rev. C* **92**, 054606 (2015). <https://doi.org/10.1103/PhysRevC.92.054606>
- [23] Shruti, Amit, C. Sharma, Subodh, N. Saneesh, K. Chakraborty, D. Arora, A. Kaur, Vikas, M. Kumar *et al.*, Study of fusion-fission dynamics of  $^{32}\text{S}+^{198}\text{Pt}$  reaction using neutron multiplicity as a probe, *Proceedings of the DAE Symp. on Nucl. Phys.*, **66**, 345 (2022). <https://sympnp.org/proceedings/>
- [24] N. Saneesh, D. Arora, A. Chatterjee, N. Kumar, A. Parihari, C. Kumar, I. Ahmed, S. Kumar, M. Kumar, A. Jhingan *et al.*, Impact of multi-chance fission on fragment-neutron correlations in  $^{227}\text{Pa}$ , *Phys. Rev. C* **108**, 034609 (2023). <https://doi.org/10.1103/PhysRevC.108.034609>
- [25] A. Kumar, A. Kumar, G. Singh, B. K. Yogi, R. Kumar, S. K. Datta, M. B. Chatterjee, and I. M. Govil, Search for entrance channel effects in heavy ion induced fusion reactions via neutron evaporation, *Phys. Rev. C* **68**, 034603 (2003). <https://doi.org/10.1103/PhysRevC.68.034603>
- [26] A. Kumar, A. Kumar, G. Singh, H. Singh, R. P. Singh, R. Kumar, K. S. Golda, S. K. Datta, and I. M. Govil, Anomalous behavior of the level density parameter in neutron and charged particle evaporation, *Phys. Rev. C* **70**, 044607 (2004). <https://doi.org/10.1103/PhysRevC.70.044607>
- [27] A. Kumar, H. Singh, R. Kumar, I. M. Govil, R. P. Singh, R. Kumar, B. K. Yogi, K. S. Golda, S. K. Datta, and G. Viesti, Pre-compound neutron evaporation in low energy heavy ion fusion reactions, *Nucl. Phys. A* **798**, 1 (2008). <https://doi.org/10.1016/j.nuclphysa.2007.10.007>
- [28] P. Dubey, P. Singh, P. Garg, and A. Kumar, Exploring the influence of entrance channel on neutron multiplicity for  $^{212}\text{Rn}^*$ , *J. Radioanal. Nucl. Chem.*, **333**, 5363 (2024). <https://doi.org/10.1007/s10967-024-09537-z>
- [29] P. Dubey and A. Kumar, Re-Investigation of Entrance Channel Effects in Heavy-Ion Fusion-Fission Dynamics, *Phys. Part. Nuclei Lett.*, **22**, 242 (2025). <https://doi.org/10.1134/S1547477124702170>
- [30] P. Dubey, M. Upadhyay, M. Choudhary, N. Singh, S. Singh, A. Kumar, N. Saneesh, M. Kumar, R. Prajapati, K. S. Golda *et al.*, New experimental insights about dissipation near shell closure, *Phys. Rev. C* **112**, L011602 (2025). <https://doi.org/10.1103/xhlj-55lw>
- [31] N. K. Rai, V. Mishra, and A. Kumar, Effect of energy variation on the dissipative evolution of the system in heavy-ion fusion reactions, *Phys. Rev. C* **98**, 024626 (2018). <https://doi.org/10.1103/PhysRevC.98.024626>
- [32] Ye Wei, Influence of Neutron Shell Closure ( $N_c=126$ ) on Prescission Particle Emission of Fissioning Systems  $^{216,224}\text{Th}$ , *Chin. Phys. Lett.* **20**, 482 (2003). <https://doi.org/10.1088/0256-307X/20/4/312>
- [33] W. Ye, Effects of the N/Z of fissioning systems on the multiplicity of pre-scission particles, *Eur. Phys. J. A*, **18**, 571 (2003). <https://doi.org/10.1140/epja/i2003-10100-9>
- [34] M. T. Senthil Kannan, J. Sadhukhan, B. K. Agrawal, M. Balasubramaniam, and S. Pal, Dynamical model calculation to reconcile the nuclear fission lifetime from different measurement techniques, *Phys. Rev. C* **98**, 021601(R) (2018). <https://doi.org/10.1103/PhysRevC.98.021601>